Thickness Effect on Mode I Trans-laminar Fracture Toughness of Quasi-isotropic Carbon/Epoxy Laminates

Xiaodong Xu*, Aakash Paul and Michael R. Wisnom

Bristol Composites Institute (ACCIS), University of Bristol, University Walk, Bristol BS8 1TR, UK

ABSTRACT

The thickness dependency of trans-laminar fracture toughness was studied in centre-notched quasi-isotropic IM7/8552 carbon/epoxy laminates with central double 0° plies with thicknesses between 1 and 8 mm. A reduction in trans-laminar fracture toughness with thickness was measured experimentally in the specimens with a 25.4 mm notch. For specimens with a shorter 12.7 mm notch, no significant dependency on specimen thickness was found. The thickness dependency was captured in detailed Finite Element models with cohesive interface elements for sub-critical damage and a Weibull criterion for fibre breakage. The reason for the thickness dependency is explained through the damage states of the individual plies which determine whether or not premature fracture occurs before the damage process zone is fully developed.

Keywords Laminates; Fracture toughness; Stress concentrations; Finite element analysis (FEA); Thickness effect

* Corresponding author. Tel.: +44 (0)117 33 15796.
E-mail address: xiaodong.xu@bristol.ac.uk (X. Xu)

1. INTRODUCTION

Trans-laminar fracture toughness is an important material property for composite structures. Composite components are often thick, but laboratory composite coupons are typically cut from thin plates. For metallic materials, fracture toughness depends on specimen thickness, with thick specimens being less tough [1, 2]. This is because the constraint provided by the thick specimen promotes a plane-strain stress state, leading to a smaller plastic zone than that in thin specimens [3]. For composite materials, the specimen thickness effect is not clear. ASTM standards are available for the measurement of fracture toughness [4, 5]. The ASTM E399 standard [4] specifies the minimum specimen thickness for metallic coupons. By comparison, the ASTM E1922 standard [5] does not specify the specimen thickness for composite materials, and only suggests that a thickness as small as 2 mm works well [5]. In fact, there is no mention of whether the measured trans-laminar fracture toughness may depend on the laminate thickness.

Few experimental studies have been conducted on the laminate-thickness dependency of trans-laminar fracture toughness. Harris and Morris [6] compared the fracture toughness values for T300/5208 graphite/epoxy quasi-isotropic laminates of different thicknesses with a fixed crack-to-width ratio of 0.5 and a 25.4 mm centre notch. They concluded that the trans-laminar fracture toughness is lower for thicker compared with thinner specimens, with a transition between 32 and 64 plies. The thickness effect was attributed to the constraint from the laminate thickness which can suppress delaminations and reduce the size of the damage process zone. Li et al. [7] reported a similar trend, i.e. a decrease in trans-laminar fracture toughness of IM7/8552 carbon/epoxy $[45/90/-45/0]_{ns}$ quasi-isotropic laminates with a 33 mm edge notch, but in

this case a reduction between 16 plies and 32 plies. Neither thicker 64-ply laminates nor thinner 8-ply laminates were tested. Li et al. [7] also reported a slight decrease of fracture energy for $[0/90]_{ns}$ cross-ply laminates between 16 plies and 32 plies. It was concluded that the thickness effect on both dispersed and blocked ply cases could not be easily explained and further investigations were needed. Laffan et al. [8] tested T300/920 carbon/epoxy cross-ply laminates of two thicknesses with a 26 mm edge notch. They found that the 34-ply $[(90/0)_8/90]_s$ laminate is tougher than the 66-ply $[(90/0)_{16}/90]_s$ laminate. No firm conclusion was drawn regarding the thickness dependency.

In this paper, trans-laminar fracture toughness is measured in centre-notched quasi-isotropic IM7/8552 carbon/epoxy laminates with central double 0° plies with two notch lengths. The specimen thicknesses vary between 8 plies (1 mm) and 64 plies (8 mm). A laminate-thickness dependency of trans-laminar fracture toughness has been found with a 25.4 mm notch, which is consistent with the findings in the literature [6-8]. The thickness effect has been influenced by the current stacking sequence which has double 0° plies at the specimen mid-plane, and the fact that the damage process zone is fully developed before ultimate failure with a 25.4 mm notch. By comparison, no significant laminate-thickness dependency was found with the shorter 12.7 mm notch, because of early unstable fracture occurring before the damage process zone is fully developed. The effect of laminate thickness in these sharp notched quasi-isotropic laminates has been successfully predicted. To the authors' best knowledge, this has not been done in the past. The reasons were explained through the predicted sub-critical damage including 0° splits.

Previous studies [7, 9, 10] focused on in-plane strength scaling in quasi-isotropic IM7/8552 carbon/epoxy laminates with a constant laminate thickness of 4 mm. The current experimental and numerical work also covers different laminate thicknesses at various specimen sizes and notch lengths, which is key for demonstrating the failure prediction capability for large and thick composite structures. A coherent explanation of the thickness effect has been provided. The current results are compared to those reported by Harris and Morris [6].

2. EXPERIMENTAL STUDY

2.1 Test configuration

A series of centre-notched quasi-isotropic IM7/8552 carbon/epoxy specimens as shown in Figure 1 with different specimen thicknesses were tested under tension. Another set of larger specimens with doubled centre-notch length and specimen width were also tested, leaving the notch-to-width ratio constant at 0.2. The tested specimen dimensions are summarized in Table 1. The crack tips are the same for all specimens, which were sharpened manually with 0.25 mm-wide piercing saw blades. The 25.4 mm centre-notched specimens have their gauge length of 254 mm kept the same as the 12.7 mm centre-notched specimens. For the shorter specimens, the closer boundaries in the length direction were previously proven not to affect the stress distribution near the notches [9].

The material used for all experiments was Hexcel's HexPly® IM7/8552 carbon/epoxy pre-preg with a nominal ply thickness of 0.125 mm. Four quasi-isotropic stacking sequences were tested with a 25.4 mm notch, which are 8-ply $[45/90/-45/0]_s$, 16-ply $[45/90/-45/0]_{2s}$, 32-ply $[45/90/-45/0]_{4s}$ and 64-ply $[45/90/-45/0]_{8s}$. The nominal laminate thicknesses are consequently 1 mm, 2 mm, 4 mm and 8 mm respectively,

which are very close to the measured specimen thicknesses. For the specimens with a 12.7 mm notch, four thicknesses with the same stacking sequences, namely, 8-ply, 16-ply, 32-ply and 64-ply were also tested. Hydraulically driven test machines were used for the experiments under displacement control at a rate of 2 mm/min.

2.2 Test results

The load vs. cross-head displacement curves are linear prior to sudden final failure in all tests. A small load drop could be seen in some tests prior to final failure due to sub-critical damage. The failure load was taken from the peak load in all tests. The Mode I trans-laminar fracture toughness is determined according to Equation 1.

$$K_{\mathrm{C}} = \sigma_{\mathrm{n}} f(\lambda)\sqrt{\frac{\pi C}{2}} \tag{1}$$

where K_{C} is the trans-laminar fracture toughness, σ_{n} is the average nominal gross section failure stress, $\lambda = C/2W = 0.1$ is the half notch-to-width ratio, C is the initial notch length, W is the specimen width and $f(\lambda) = \sqrt{\sec(\pi\lambda)}$ is a geometrical parameter to account for the effect of finite width and is equal to 1.025 for this case [11].

This equation was used for convenience, and is fine for comparison purposes, although it has been shown that the size of the damage process zone should really be accounted for in determining the true trans-laminar fracture toughness [12].

Table 2 presents the test results. The measured trans-laminar fracture toughness decreases from the thinnest laminates with a 25.4 mm notch to the thickest laminates by 12%. The difference is statistically significant with a 95% level of confidence based on the Student's t-test. In contrast, the measured fracture toughness does not show a significant thickness dependency for the 12.7 mm notch.

3. NUMERICAL STUDY

3.1 Ply-by-ply detailed FE analysis with cohesive interface elements

A detailed FE analysis with the explicit software LS-Dyna was conducted to investigate the laminate-thickness effects. Individual plies were modelled with cohesive interface elements to model potential splits within plies and the delaminations between adjacent plies. The splits and delaminations can significantly influence the trans-laminar fracture toughness. The nominal ply thickness of 0.125 mm is represented by one 8-node continuum element through the specimen thickness. A typical in-plane FE mesh is shown in Figure 2. It was reported in Ref. [13] that if the tip radius is smaller than 0.5 mm in quasi-isotropic IM7/8552 carbon/epoxy laminates, the crack is sharp enough to not affect measured trans-laminar fracture toughness. A triangular shaped sharp notch tip could therefore be modelled, with the much smaller tip radius than in the tests not expected to affect the results.

Previously, it was found that multiple potential split paths need to be pre-defined in the 0° plies, to simulate the progressive damage process zone development at the notch tip [10]. If the 0° split spacing is not larger than 1 mm, the results are not sensitive to the split spacing [10]. There was only a single pre-defined potential split path in the plies with other orientations (±45° and 90°), starting from each notch tip. This was previously shown to be adequate, with the notched behaviour predicted satisfactorily for 32-ply (4 mm) laminates as fibre breakage was confined within the initial splits [10]. The previous study also showed that when the mesh size at the notch tips is no more than 0.2 mm, the results are not very sensitive to the mesh size [10].

In the current FE models, there are a total of 9 pre-defined potential 0° split paths (marked in red) over a distance of 4 mm from the notch tip in the typical FE mesh in

Figure 2. The consequent split spacing is 0.5 mm. A minimum mesh size of about 0.1 mm was arranged near the notch tips within the ±45° lines to simulate the progressive damage process zone development. A slightly coarser mesh was used outside this region. The properties for the detailed ply-by-ply modelling listed in Table 3 [14] were measured from independent characterisation tests except for the strengths of the cohesive interface elements, which are not critical, as shown later. The mixed-mode traction separation relationship for the cohesive interface elements is shown in Figure 3 [15].

A criterion based on Weibull statistics has been used to simulate fibre failure [16]. Assuming equal probability of survival between the model and a unit volume of material, we have Equation 2 [17], which is checked at each time step in the explicit FE analysis.

$$\sum_{i=1}^{\text{Total Number of Elements}} V_i (\sigma_i / \sigma_{\text{unit}})^m = 1 \qquad (2)$$

where, σ_i is the elemental centroidal stress in the fibre direction, V_i is the elemental volume, $\sigma_{\text{unit}} = 3131$ MPa is the tensile strength of a unit volume of material and $m = 41$ is the Weibull modulus of the material [14].

When Equation 2 is satisfied, the element with the maximum fibre-direction elemental stress loses its load carrying capability and its contribution is removed. The process repeats and interacts with the development of multiple 0° splits, which can represent the progressive fibre breakage process within the damage process zone [10].

3.2 Damage states in detailed FE models

By combining the cohesive interface elements and the Weibull fibre failure criterion, the current detailed models can predict closely the damage states within the individual plies in the laminates with different thicknesses from 1 mm to 8 mm. Taking a 4 mm-thick 12.7 mm centre-notched model for example, the damage states in the individual plies including splitting, delamination and fibre fracture before ultimate failure agree well with

the X-ray Computed Tomography (CT scan) images taken at 95% of the average failure load, as shown in Figure 4. The same detailed modelling technique was also used to model the centre-notched specimens with different specimen thicknesses and different notch lengths.

The predicted damage states are different between the outboard single 0° plies and the central double 0° ply. For example, in the 4 mm-thick 12.7 mm centre-notched model in Figure 4, the damage in the central double 0° ply (Figure 4(a)) is greater than that in the outboard single double 0° ply (Figure 4(b)) in terms of the extent of splitting and the shape of delamination. The predicted maximum split lengths in the 0° plies of the different models just before ultimate failure are summarised in Table 4. On average, the predicted maximum 0° split lengths is about 33% lower in the single compared with double 0° plies. The predicted maximum 0° split lengths in all plies are similar between the 4 mm-thick 12.7 mm centre-notched model and 25.4 mm centre-notched model.

The central double 0° ply was found to break later than the outboard single 0° plies due to longer double 0° splitting e.g. in the 3.2 mm centre-notched tests, no fibre breakage was observed in the central double 0° ply at 95% of the average failure load with the outboard single 0° plies already broken [9]. Therefore, the ultimate failure of the centre-notched laminate is postulated to be triggered by the unstable fracture propagation in the double 0° ply. Hence, the damage state including splitting in the double 0° ply is a particular focus of the current study.

3.3 Notch length effects

The unstable fracture of the central double 0° ply is affected by the 0° splitting, which depends on the notch length. If the 0° split lengths are normalised by the notch lengths, the normalised maximum 0° split lengths are much larger in the 4 mm-thick 12.7

mm centre-notched model (0.87 in the double 0° ply) than in the 25.4 mm centre-notched model (0.42 in the double 0° ply) as listed in Table 4. This has some important implications for the different thickness dependency between the 12.7 mm and 25.4 mm centre-notched models, as discussed later.

According to Ref. [10], the growth of the 0° splits is driven by the available energy, and the Stress Concentration Factors (SCFs) decrease with increasing normalised 0° split lengths. This is now demonstrated by a simpler 12.7 mm centre-notched model without considering fibre fracture as shown in Figure 5. The purpose is to address the effect of the central double 0° splits on equavilent SCFs. In Figure 5, the maximum fibre-direction elemental stress in the central double 0° plies is converted to an equivalent value for the laminate by dividing a factor of 2.61 which is the ratio between the stress in the 0° ply and the average stress in the laminate according to Classical Laminate Theory (CLT). Then the equivalent stress in the laminate is divided by the applied gross-section stress to calculate the equivalent SCFs. As the applied load and hence the available energy increases, the central double 0° splits grow and the equivalent SCFs decrease as shown in Figure 5. As demonstrated by the two schematics in Figure 5, the rate of equivalent SCF reduction also decreases as the normalised 0° splits grow, until the equivalent SCFs no longer change significantly in the central double 0° ply. The two normalised split lengths of the schematics are from the predicted maximum central double 0° split lengths in Table 4 (0.42 for the 25.4 mm notch and 0.87 for the 12.7 mm notch).

Using the curve from Figure 5 together with the schematics in Figure 6, we can qualitatively describe how equivalent SCFs change after effective crack increments in the 0° plies of the current detailed FE model. When the stress is high enough at the notch tip, fibre failure will occur in the 0° plies. Then the extended crack arrests after gaining an

effective crack increment of Δa, and a new secondary 0° split grows at the newly formed crack tip. The new secondary 0° split is predicted to be longer than the initial 0° split after the crack increment ($S_1 > S_0$). But the crack length has also increased. The important point is what happens to the normalised 0° split (secondary 0° split length S_1 divided by the notch length a_1) as the crack grows further. With a longer 25.4 mm notch according to Figure 6(a), this can result in stable fracture at the same applied load because the equivalent SCF is lower at a larger nominalised split length ($SCF_1 < SCF_0$). As a result, the damage process zone can grow stably until it approaches its full size. It was previously defined that the damage process zone is the area where the 0° plies are broken, but some ±45° plies are intact, with size determined from the distance between the last 0° split at the newly formed crack tip and the initial notch tip [9]. When all the 0° and ±45° plies break, the damage process zone is fully developed [18]. This was previously confirmed when it was found that the damage process zone approaches a constant size before ultimate failure in the specimens with a centre notch of at least 25.4 mm [9]. In the current study, the predicted damage process zone is similarly believed to reach its full size with a 25.4 mm centre notch. It is also because some -45° plies are predicted to break before ultimate failure. After the damage process zone is fully developed, Δa is equal to the size of the fully developed damage zone. Fracture through the full thickness will occur unstably with further crack increments.

We can also qualitatively explain the reason why ultimate failure can sometimes occur even before the damage process zone is fully developed. With a shorter 12.7 mm notch as shown in Figure 6(b), the equivalent SCF is no longer significantly reduced ($SCF_1 \approx SCF_0$) when the already long normalised 0° split grows further after the crack increment ($S_1 > S_0$). Having a similar equivalent SCF ($SCF_1 \approx SCF_0$) as the crack grows further can

lead to unstable crack propagation at the same applied load. This occurs when the new secondary 0° split is still growing, but before the damage process zone is fully developed. The effect will be even more pronounced for smaller notches where the normalised split lengths will be even greater. This explains why if the specimen is too small, premature failure occurs before the damage process zone is fully developed and the apparent trans-laminar fracture toughness is lower.

3.4 Specimen thickness effects

Because the detailed FE models capture closely the different damage states in the individual plies of the centre-notched models, the FE results correlate with the experimental results, as shown in Figure 7. The predicted and measured notch strengths decrease significantly as the specimen thicknesses increase in the 25.4 mm centre-notched specimens. In contrast, the predicted notched strengths remain approximately constant for the 12.7 mm centre-notched specimens. The predicted trans-laminar fracture toughness values are calculated according to Equation 1 based on the predicted notch strengths. They are compared against the measured values in Table 5.

For the laminates with a 25.4 mm notch, the damage process zone was found to approach its full size [9], and there is a laminate-thickness dependency of the trans-laminar fracture toughness. The central double 0° ply tends to be tougher than the outboard single 0° plies because of more sub-critical damage i.e. longer central 0° splits which lead to lower equivalent SCFs or more stress blunting as shown in Figure 6(a). This results in a tougher response in the thinner specimens which have a relatively larger proportion of double 0° plies. For example, a 1 mm-thick laminate has 100% double 0° plies. But as the specimen gets thicker, the central double 0° ply represents a relatively smaller proportion, e.g. only 12.5% in an 8 mm-thick laminate, and so their contribution gradually reduces.

The notched strength of very thick specimens therefore is determined mainly by the single 0° plies and becomes independent of the laminate thickness.

In contrast, in the 12.7 mm centre-notched model, the normalised double 0° splits are much longer than those in the 25.4 mm centre-notched model as shown in Table 4. Due to the longer 0° splits relative to the notch length, further increasing the split length in the central double 0° dominated thin model can no longer effectively reduce the equivalent SCFs, i.e. longer central double 0° splits do not necessarily lead to lower equivalent SCFs nor more stress blunting as shown in Figure 6(b). The approximately constant equivalent SCF after further crack growth can lead to unstable crack propagation in the central double 0° ply. This results in early unstable fracture in the double 0° dominated thin model with a 12.7 mm notch before the damage process zone is fully developed, which undermines the thickness dependency seen with the 25.4 mm notch. The predicted strength increases slightly from 1 to 2 mm thickness in the 12.7 mm centre-notched model because the 1 mm-thick model sees premature unstable failure with only one central double 0° ply through the model thickness. The instability existing in the central double 0° ply before the damage process zone is fully developed may also explain the larger experimental scatter in the thin-laminate tests.

4. DISCUSSION

Harris and Morris [6] reported that thicker 25.4 mm centre-notched quasi-isotropic laminates have lower trans-laminar fracture toughness values, as shown in Figure 8. It was concluded that the thickness effect is caused by the constraint on the damage process zone in the thick specimens, minimizing internal delaminations and limiting the size of the damage process zone. It may be plausible for the $[0/\pm45/90]_{ns}$ stacking sequence, as there are 0° plies on the surfaces where the sub-critical damage is

the most and the constraint is the least. However, it cannot explain the laminate-thickness effect in the current IM7/8552 carbon/epoxy $[45/90/-45/0]_{ns}$ laminates, because the sub-critical damage in the 0° plies is also very large at the specimen centre where any constraint due to the specimen thickness is expected to be the greatest. Alternatively, if the thickness effect is explained based on the damage states in the individual plies, the results for both the current layup and the previous stacking sequence used in Harris and Morris [6] can be explained coherently. The sub-critical damage in the surface 0° ply which has less constraint from the adjacent plies will behave similarly to that in the central double 0° ply which has more energy available to drive splits and delaminations. Different proportions of the surface 0° plies with greater sub-critical damage in specimens of different thicknesses lead to the laminate-thickness effects. Our observed trend is consistent with these findings in Ref. [6], all based on quasi-isotropic 25.4 mm centre-notched specimens.

Laffan et al. [8] found the same thickness dependency with thinner cross-ply laminates being tougher (28% at initiation and 14% at propagation), but no explanation was given. It should be noted that the cross-ply laminates behave differently from the quasi-isotropic laminates in terms of the damage process zone development. For example, Harris and Morris [6] stated that cross-ply laminates are more susceptible to 0° splitting. Compared to quasi-isotropic laminates, cross-ply laminates also do not contain ±45° plies which influence the damage zone development [18]. Therefore, further work is required to establish the more general thickness dependency.

The parameters in Table 3 have been previously applied to different FE model configurations (e.g. open-hole, centre-notched and over-height compact tension specimens), widths (16 to 254 mm) and thicknesses (1 to 8 mm) [10, 14, 17] and shown to

be valid. The predicted centre-notch tensile strength is not sensitive to the strengths of the cohesive interface elements, because it is controlled by damage propagation rather than initiation, which occurs early on due to the stress concentration at the notch tip. For instance, when a strength combination of 111 MPa for Mode I and 120 MPa for Mode II [19] is used instead of 60 MPa for Mode I and 90 MPa for Mode II, the predicted tensile strength for 4 mm-thick 12.7 mm centre notch is only 0.6% lower.

Some recommendations can be given for trans-laminar fracture toughness testing for composite laminates in addition to those in ASTM E1922 standard [5]. First, the notch length should be large enough to be able to generate a fully developed damage process zone, so that the measured trans-laminar fracture toughness can represent a material property. For the current IM7/8552 carbon/epoxy material and layup with the centre-notch specimen configuration, the notch length should be at least 25.4 mm. Second, the specimen should be thick enough to be able to generate a trans-laminar fracture toughness value that is independent of the specimen thickness and conservative. For the current configuration, the minimum specimen thickness should be 4 mm.

5. CONCLUSIONS

The Mode I trans-laminar fracture toughness measured using 25.4 mm centre-notched specimens demonstrates a laminate-thickness dependency from 8-ply laminates (1 mm) to 64 plies (8 mm) for IM7/8552 carbon/epoxy $[45/90/-45/0]_{ns}$ laminates. The thinner laminates are tougher than the thicker ones. In contrast, the measured trans-laminar fracture toughness from the test results with a 12.7 mm notch does not show the same thickness dependency, and the trans-laminar fracture toughness values are lower than with the longer notch.

The thickness dependency of Mode I trans-laminar fracture toughness for the centre-notched specimens was successfully captured by the detailed FE models with cohesive interface elements for delamination and splitting and a Weibull failure criterion for fibre breakage. The laminate-thickness dependency of trans-laminar fracture toughness was explained through the detailed damage states in the individual plies. For the current quasi-isotropic stacking sequence, the double 0° ply at the specimen mid-plane promotes more sub-critical damage such as splits and delaminations. Consequently, the double 0° splitting can significantly blunt the stress concentrations. This leads to a tougher response of the central double 0° ply provided the damage process zone is fully developed before ultimate failure, which is the case with a 25.4 mm notch. Specimens of different thicknesses have different proportions of the central double 0° ply, which results in the laminate-thickness dependency of trans-laminar fracture toughness.

The lack of significant thickness dependency in the 12.7 mm notched tests was also successfully captured by the detailed FE models. This is because the 12.7 mm centre-notched models have much greater normalised 0° split lengths than the 25.4 mm centre-notched models. The additional stress blunting effect due to the longer normalised central double 0° splits is no longer significant with further split growth after crack increments. This can lead to unstable fracture of the central double 0° ply, and hence early unstable fracture in the central double 0° ply dominated thin laminates before the damage process zone is fully developed. Consequently, the thickness dependency seen with a 25.4 mm notch does not arise with a 12.7 mm notch. This also explains more generally why specimens with small notches may fail before the damage process zone is fully developed, and therefore exhibit lower apparent trans-laminar fracture toughness.

The same thickness dependency has been reported in other quasi-isotropic stacking sequences with surface 0° plies. This can be explained according to the current study because the surface 0° plies which lack constraint from the adjacent plies have the same influence on trans-laminar fracture toughness as the double central 0° ply. Some cross-ply laminates have also demonstrated similar thickness dependency, but further studies are required to understand the effects more generally in other laminates.

DATA AVAILABILITY

The data required to support the conclusions are provided in the results sections of this paper.

REFERENCES

[1] Broek D. Elementary engineering fracture mechanics. Fourth revised ed. London: Kluwer Academic Publishers, 1986.

[2] Markstrom K. On fracture toughness and its size dependence for steels showing thickness delamination. Engineering Fracture Mechanics. 1972;4:593-603.

[3] Broek D. The practical use of fracture mechanics: Kluwer Academic Publishers, 1989.

[4] ASTM, Standard, E399-90. Standard test method for plane-strain fracture toughness of metallic materials. West Conshohocken, PA, USA: ASTM International; 1990 (1997).

[5] ASTM, Standard, E1922-97. Standard test method for translaminar fracture toughness of laminated polymer matrix composite materials. West Conshohocken, PA, USA: ASTM International; 1997.

[6] Harris CE, Morris DH. Effect of laminate thickness and specimen configuration on the fracture of laminated composites. Composite Materials: Testing and Design (Seventh Conference). 1986;ASTM STP 893:117-95.

[7] Li X, Hallett SR, Wisnom MR, Zobeiry N, Vaziri R, Poursartip A. Experimental study of damage propagation in Over-height Compact Tension tests. Composites Part A: Applied Science and Manufacturing. 2009;40:1891-9.

[8] Laffan MJ, Pinho ST, Robinson P, Iannucci L. Measurement of the in situ ply fracture toughness associated with mode I fibre tensile failure in FRP. Part II: Size and lay-up effects. Composites Science and Technology. 2010;70:614-21.

[9] Xu X, Wisnom MR, Mahadik Y, Hallett SR. An experimental investigation into size effects in quasi-isotropic carbon/epoxy laminates with sharp and blunt notches. Composites Science and Technology. 2014;100:220-7.

[10] Xu X, Wisnom MR, Li X, Hallett SR. A numerical investigation into size effects in centre-notched quasi-isotropic carbon/epoxy laminates. Composites Science and Technology. 2015;111:32-9.

[11] Newman JC. Fracture analysis of various cracked configurations in sheet and plate materials. Properties Related to Fracture Toughness ASTM STP 605. 1976:104-23.

[12] Xu X, Takeda S, Aoki Y, Hallett SR, Wisnom MR. Predicting notched tensile strength of full-scale composite structures from small coupons using fracture mechanics. Composite Structures. 2017;180:386-94.

[13] Camanho PP, Catalanotti G. On the relation between the mode I fracture toughness of a composite laminate and that of a 0° ply: Analytical model and experimental validation. Engineering Fracture Mechanics. 2011;78:2535-46.

[14] Hallett SR, Green BG, Jiang WG, Wisnom MR. An experimental and numerical investigation into the damage mechanisms in notched composites. Composites Part A: Applied Science and Manufacturing. 2009;40:613-24.

[15] Jiang W-G, Hallett SR, Green BG, Wisnom MR. A concise interface constitutive law for analysis of delamination and splitting in composite materials and its application to scaled notched tensile specimens. International Journal for Numerical Methods in Engineering. 2007;69:1982-95.

[16] Wisnom MR. Size effects in the testing of fibre-composite materials. Composites Science and Technology. 1999;59:1937-57.

[17] Li X, Hallett SR, Wisnom MR. Numerical investigation of progressive damage and the effect of layup in overheight compact tension tests. Composites Part A: Applied Science and Manufacturing. 2012;43:2137-50.

[18] Xu X, Wisnom MR, Mahadik Y, Hallett SR. Scaling of fracture response in over-height compact tension tests. Composites Part A: Applied Science and Manufacturing. 2015;69:40-8.

[19] Charalambous G, Allegri G, Lander JK, Hallett SR. A cut-ply specimen for the mixed-mode fracture toughness and fatigue characterisation of FRPs. Composites Part A: Applied Science and Manufacturing. 2015;74:77-87.

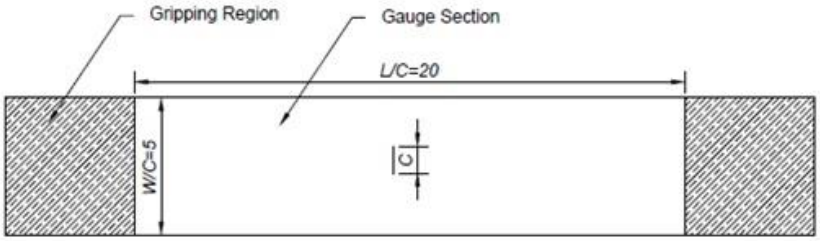

Figure 1. Schematics of the centre-notched specimen (C = 12.7 mm).

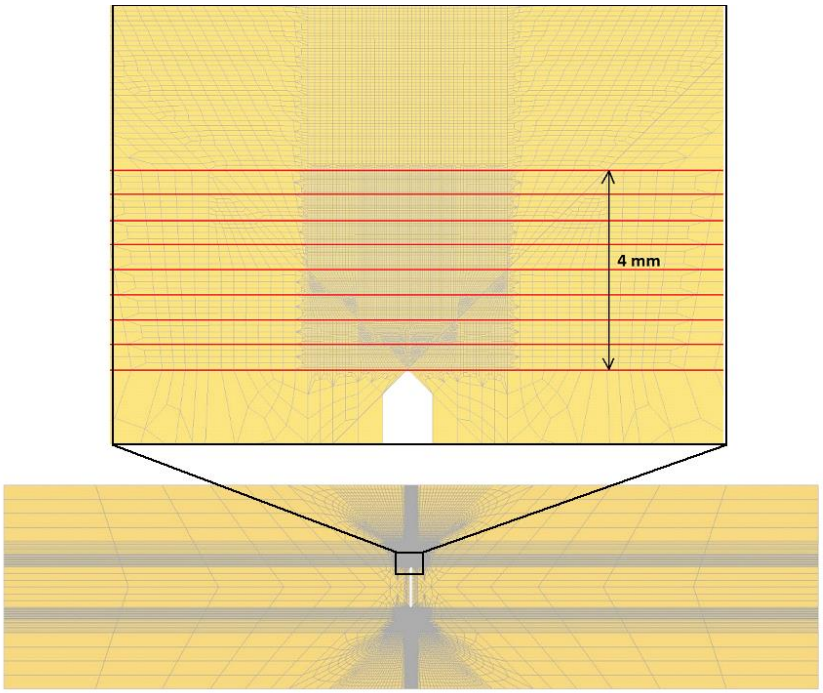

Figure 2. Typical in-plane mesh for detailed FE models in LS-Dyna with pre-defined 0° split paths for cohesive interface elements marked in red.

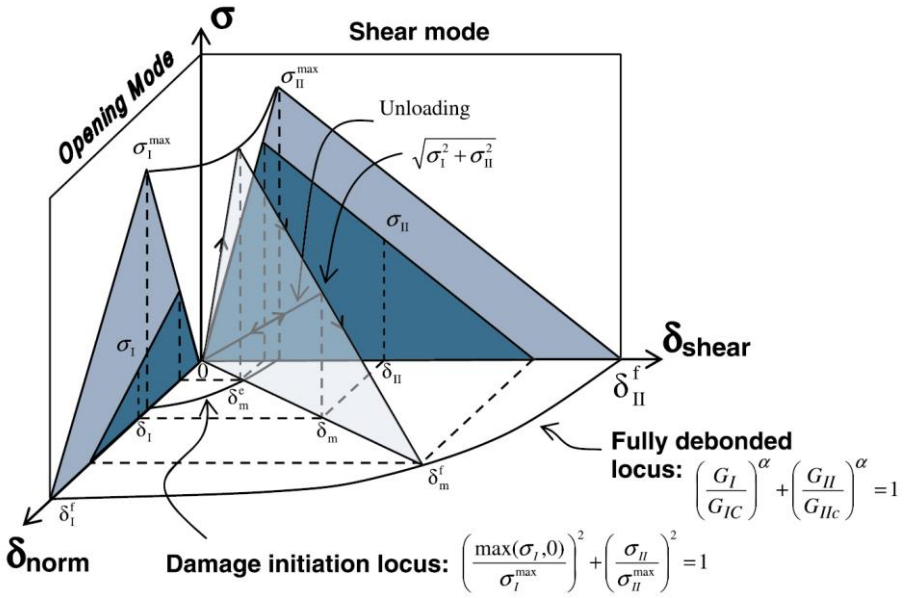

Figure 3. Mixed-mode traction separation relationship for cohesive interface elements [15].

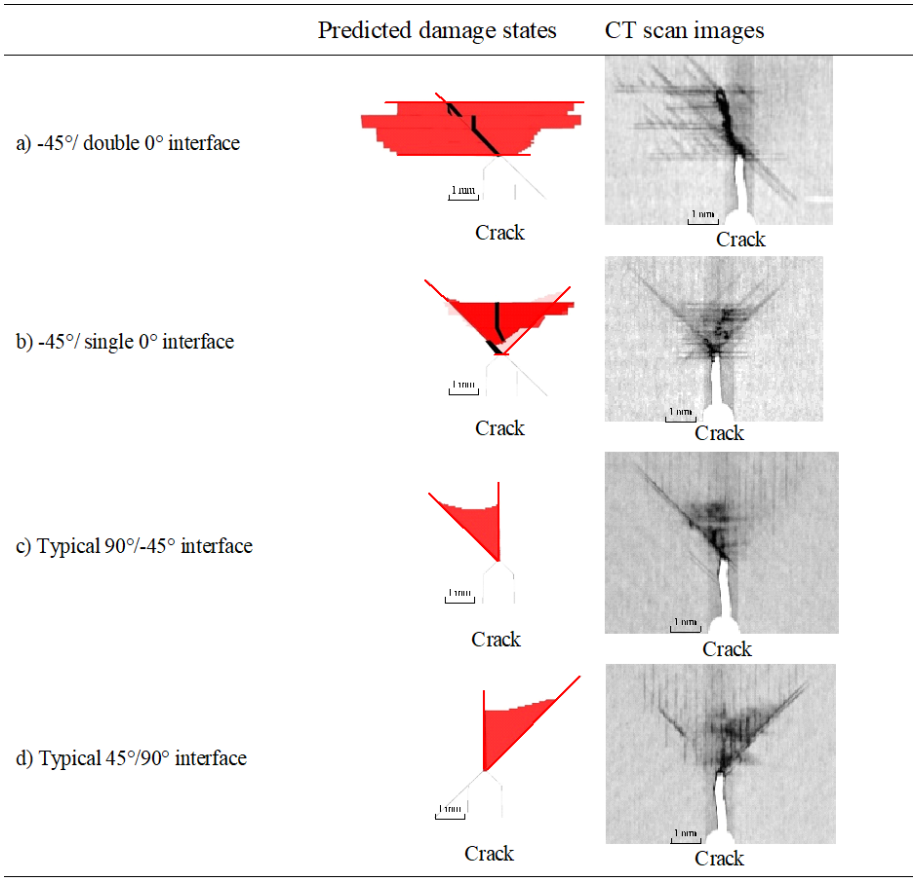

Figure 4. Damage states in individual plies in 4 mm-thick 12.7 mm centre-notched model just before ultimate failure vs. CT scan images taken at 95% of the average failure load (Sub-critical damage marked in red in the model and fibre breakage in adjacent 0° ply beneath marked in black).

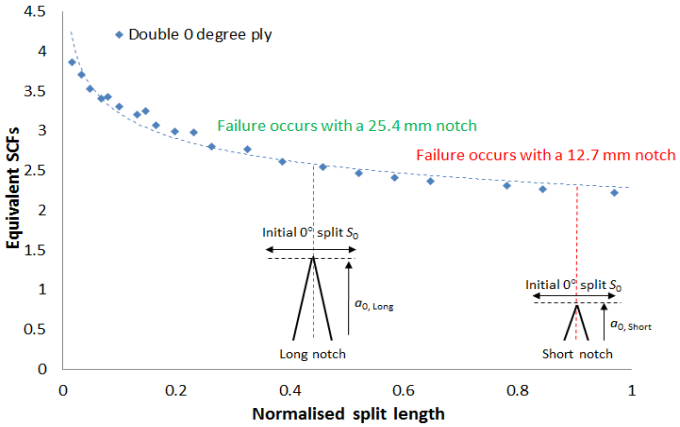

Figure 5. Equivalent SCFs decrease with normalised split lengths in the simpler model without fibre fracture.

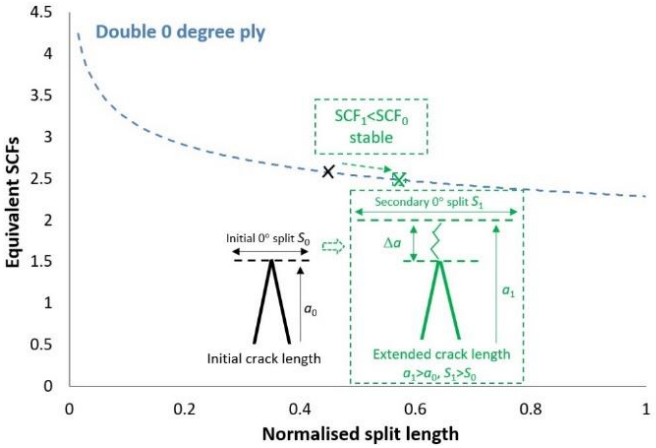

(a) Long notch

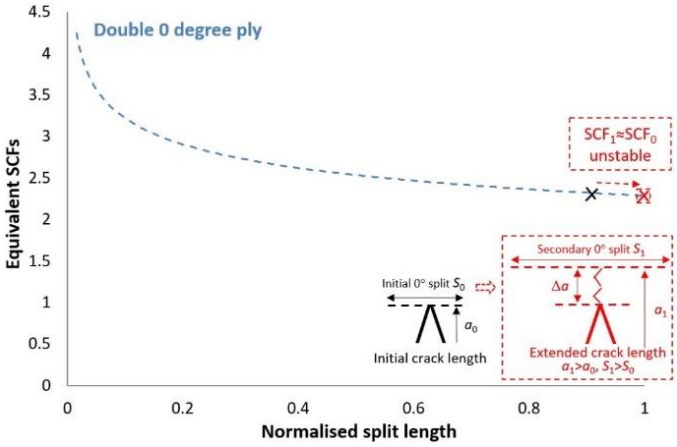

(b) Short notch

Figure 6. Failure analysis of the detailed FE models with two different notch lengths.

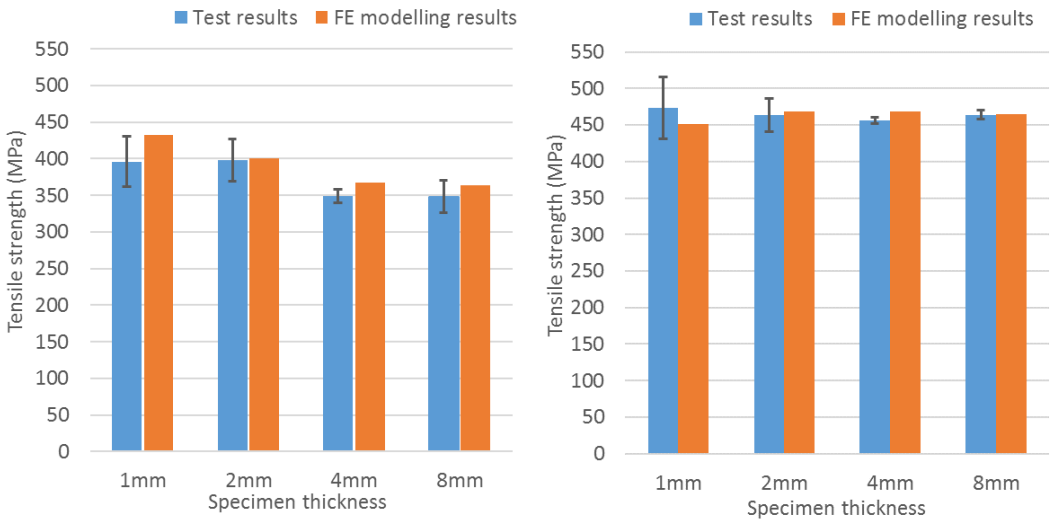

a) 25.4 mm centre-notched tests b) 12.7 mm centre-notched tests

Figure 7. Detailed modelling results correlate to experimental results with different notch lengths and laminate thicknesses.

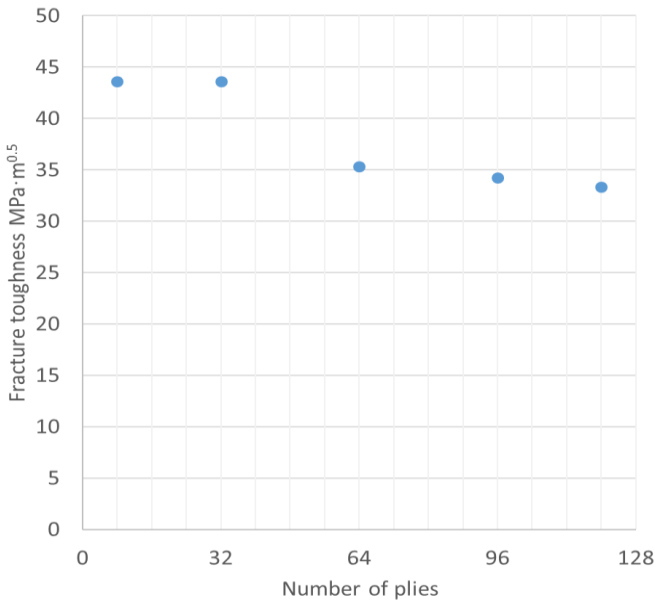

Figure 8. Specimen-thickness dependency of trans-laminar fracture toughness reported in Ref. [6].

Table 1. In-plane dimensions of centre-notched specimens [mm].

Specimens	Notch length	Gauge width	Gauge length	End tab length
Small	12.7	63.5	254.0	100.0
Large	25.4	127.0	254.0	100.0

Table 2. Summary of test results.

Notch length [mm]	Stacking sequence	No. of specimens	Tensile strength [MPa] (CV%)	Fracture toughness [MPa·m$^{1/2}$]
12.7	8-ply $[45/90/-45/0]_s$	4	474 (8.9)	69
	16-ply $[45/90/-45/0]_{2s}$	5	464 (4.9)	67
	32-ply $[45/90/-45/0]_{4s}$	5	456 (0.9) [9]	66
	64-ply $[45/90/-45/0]_{8s}$	5	464 (1.4)	67
25.4	8-ply $[45/90/-45/0]_s$	4	396 (8.6)	81
	16-ply $[45/90/-45/0]_{2s}$	4	398 (7.1)	81
	32-ply $[45/90/-45/0]_{4s}$	4	349 (2.7) [9]	71
	64-ply $[45/90/-45/0]_{8s}$	4	348 (6.3)	71

Table 3. Input parameters for detailed FE models [14].

Properties of cohesive interface elements				
G_{IC} [N/mm]	G_{IIC} [N/mm]	σ_I^{max} [MPa]	σ_{II}^{max} [MPa]	
0.2	1.0	60 [a]	90 [a]	
Properties of continuum elements				
E_{11} [GPa]	$E_{22}=E_{33}$ [GPa]	$G_{12}=G_{13}$ [GPa]	G_{23} [GPa]	m
161	11.4	5.17	3.98	41
σ_{11}^{max} [MPa]	$\alpha_{22}=\alpha_{33}$ [°C^{-1}]	α_{11} [°C^{-1}]	$\upsilon_{12}=\upsilon_{13}$	υ_{23}
3131 [b]	3×10^{-5}	0.0	0.320	0.436

[a] The strengths of the cohesive interface elements are assumed.

[b] 3131 MPa is for a unit volume of material.

Table 4. Predicted maximum 0° split length just before ultimate failure [mm].

	25.4 mm notch			12.7 mm notch		
Laminate thickness	Double 0° splitting	Single 0° splitting	Difference	Double 0° splitting	Single 0° splitting	Difference
1 mm	12.4	-	-	11.4	-	-
2 mm	10.1	6.6	35%	11.5	8.4	27%
4 mm	10.2	6.9	32%	10.9	6.8	38%
8 mm	9.7	6.6	32%	10.3	6.6	36%
Mean	10.6	6.7		11.0	7.3	
Normalised	0.42 [a]	0.26 [a]		0.87 [a]	0.57 [a]	

[a] The average 0° split lengths are normalised by notch lengths.

Table 5. Results comparison between experiment and FE analysis.

Notch length [mm]	Stacking sequence	Fracture toughness from experiment [MPa·m$^{1/2}$]	Fracture toughness from FE analysis [MPa·m$^{1/2}$]
12.7	8-ply $[45/90/-45/0]_s$	69	65
	16-ply $[45/90/-45/0]_{2s}$	67	68
	32-ply $[45/90/-45/0]_{4s}$	66	68
	64-ply $[45/90/-45/0]_{8s}$	67	67
25.4	8-ply $[45/90/-45/0]_s$	81	88
	16-ply $[45/90/-45/0]_{2s}$	81	82
	32-ply $[45/90/-45/0]_{4s}$	71	75
	64-ply $[45/90/-45/0]_{8s}$	71	75